AGU PUBLICATIONS

Geophysical Research Letters

RESEARCH LETTER
10.1002/2017GL075468

Key Points:
- Titan's seas are consistent with an equipotential surface
- The liquid elevation of Titan's lakes can be found hundreds of meters above the seas
- Lakes reside in topographically closed, sharp-edged depressions. Many have raised rims that are hard to reconcile with formation models

Supporting Information:
- Supporting Information S1

Correspondence to:
A. G. Hayes,
hayes@astro.cornell.edu

Citation:
Hayes, A. G., Birch, S. P. D., Dietrich, W. E., Howard, A. D., Kirk, R. L., Poggiali, V., … Wood, C. A. (2017). Topographic constraints on the evolution and connectivity of Titan's lacustrine basins. *Geophysical Research Letters*, *44*, 11,745–11,753. https://doi.org/10.1002/2017GL075468

Received 31 AUG 2017
Accepted 1 NOV 2017
Accepted article online 6 NOV 2017
Published online 2 DEC 2017

Topographic Constraints on the Evolution and Connectivity of Titan's Lacustrine Basins

A. G. Hayes[1], S. P. D. Birch[1], W. E. Dietrich[2], A. D. Howard[3], R. L. Kirk[4], V. Poggiali[1], M. Mastrogiuseppe[1,5], R. J. Michaelides[1,6], P. M. Corlies[1], J. M. Moore[7], M. J. Malaska[8], K. L. Mitchell[8], R. D. Lorenz[9], and C. A. Wood[10]

[1]Department of Astronomy, Cornell University, Ithaca, NY, USA, [2]Department of Earth and Planetary Sciences, UC Berkeley, Berkeley, CA, USA, [3]Department of Environmental Sciences, University of Virginia, Charlottesville, VA, USA, [4]USGS Astrogeology Science Center, Flagstaff, AZ, USA, [5]Department of Information, Electronical and Telecommunications Engineering, Sapienza University of Rome, Rome, Italy, [6]Department of Geophysics, Stanford University, Stanford, CA, USA, [7]NASA Ames Research Center, Mountain View, CA, USA, [8]Jet Propulsion Laboratory, California Institute of Technology, Pasadena, CA, USA, [9]Applied Physics Laboratory, The Johns Hopkins University, Laurel, MD, USA, [10]Planetary Science Institute, Tucson AZ, USA

Abstract The topography provided by altimetry, synthetic aperture radar-topography, and stereo radargrammetry has opened new doors for Titan research by allowing for quantitative analysis of morphologic form. Using altimetry measurements, we show that Titan's Maria are consistent with an equipotential surface but that several filled lakes are found to be hundreds of meters above this sea level, suggesting that they exist in isolated or perched basins. Within a given drainage basin, empty lake floors are typically higher than the liquid elevation of nearby lakes/seas, suggesting local subsurface connectivity. The majority of Titan's lakes reside in topographically closed, sharp-edged depressions whose planform curvature suggests lateral expansion through uniform scarp retreat. Many, but not all, empty lake basins exhibit flat floors and hectometer-scale raised rims that present a challenge to formation models. We conclude that dissolution erosion can best match the observed constraints but that challenges remain in the interpretation of formation processes and materials.

Plain Language Summary From a combination of topographic techniques, we show that the liquid elevations of Titan's seas are consistent with an equipotential surface (similar to Earth's oceans). The same measurements show that Titan's small lakes can be found several hundreds of meters above the sea level, suggesting that they are potentially isolated from the seas. Within a given watershed, however, nearby lakes show evidence for local connectivity. Using the same topographic data set, we examine the topographic profile of Titan's filled and empty lake depressions. The depressions have flat floors and hundred-meter scale raised rims that present a challenge to understanding their formation. We conclude that dissolution erosion (e.g., karst on Earth) can best match the observed constraints but that challenges still exist in the interpretation of formation processes and materials.

1. Introduction

Titan's polar terrain are dominated by smooth undulating plains, which are bounded by moderately dissected uplands that separate the surface into discretized topographic basins (Birch et al., 2017; Moore et al., 2014). Insets into the undulating plains and dissected uplands are broad (low sloping, diffuse perimeters) and sharp-edged (steep-sided perimeters) depressions, which are found with varying amounts of liquid fill (dry, partially filled, and inundated; Hayes et al., 2008, Hayes, 2016). Liquid-filled broad depressions contain Titan's largest lacustrine bodies, including the seas Ligeia Mare, Kraken Mare, and Punga Mare, as well as the larger lakes, including Jingpo Lacus and Bolsena Lacus. In the south polar region, dry broad depressions have been identified as putative paleo seas (Birch et al., 2017; Hayes et al., 2011) that display evidence of having been filled during an earlier epoch (Aharonson et al., 2009). The sharp-edged depressions (henceforth referred to as SEDs) are steep-sided depressions defined by high sloping walls, relative to the surrounding undulating plains, that generate layover and incidence angle effects in synthetic aperture radar (SAR) images (see Figure 1). SEDs include the majority of Titan's smaller lakes and are morphologically distinct from the larger, broad depressions (Hayes, 2016). The morphologic similarities between filled and empty SEDs have been used to suggest that dry SEDs represent previously filled, but now empty, lakes (Hayes et al.,

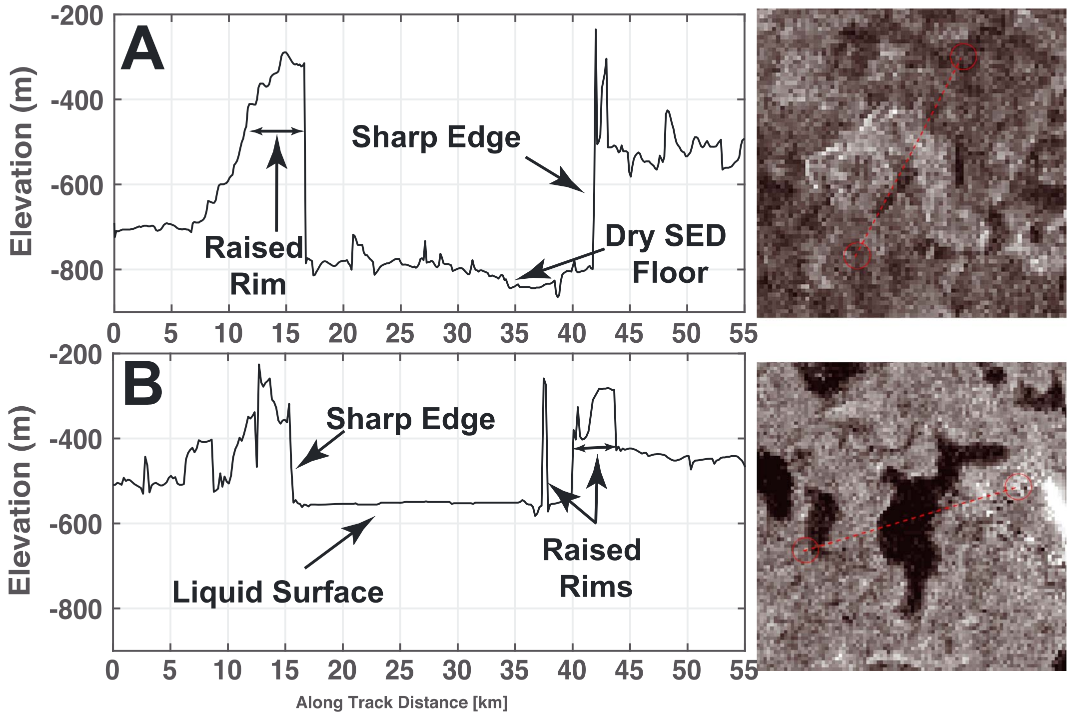

Figure 1. Closest-approach altimetry profiles an unfilled and filled SED observed in (a) May 2007 (T30) and (b) April 2017 (T126), respectively. The profiles were processed to improve along-track resolution using the delay-Doppler algorithm described in Michaelides et al. (2016). Note that raised rims border the steep-sided depressions in both the empty and filled SEDs.

2008). The spatial ubiquity and distinct morphologic expression of the SEDs make them a distinctive landform of Titan's polar terrain (e.g., Aharonson et al., 2014).

While Titan's larger lakes and seas appear to have developed in part through inundation of a preexisting well-drained landscape, producing morphologic signatures consistent with drowned topography (Stofan et al., 2007), the smaller lakes, which have a median diameter of 77 ± 20 km (Hayes et al., 2008) and primarily consist of liquid-filled SEDs (Birch et al., 2017), appear to originate through different processes. SED formation, both dry and filled, is not well understood, and the topographic data necessary to constrain potential mechanisms (e.g., Corlies et al., 2017) have only recently become available. Herein, we perform a survey of the three-dimensional morphometric properties of Titan's SEDs that can be used to further evaluate current formation hypothesis and/or generate new ones. The goal of this work is not to uniquely determine the formation mechanisms responsible for generating the SEDs but rather to provide a list of observables that will constrain and guide formation theories. SEDs are geomorphologically unique and may represent a linchpin to understand the formation and subsequent evolution of Titan's polar terrains.

2. Establishing a Reference Datum: Liquid Elevation of Titan's Mare

The three-dimensional relationships among geomorphic units can be used to reveal the history of a landscape and provide insight into the process interactions that drive its evolution (e.g., Dietrich et al., 2013). We exploit this interrelationship to study constraints on lacustrine basin structure and formation in Titan's polar landscapes. Our analysis uses topographic maps from Corlies et al. (2017), which uses a combination of all available altimetry, SAR-Topography (SAR-Topo), and radargrammetry data products, and includes a global minimization of the relative offsets between these products. Liquid elevations are retrieved from eight altimetry passes (Figure S1 in the supporting information) that intersect Titan's north and south polar regions (defined as being poleward of 55°). SAR-Topo products, through July 2016 (T121), cover 8.1% of the north and 8.2% of the south, while the available radargrammetry-derived digital topographic models encompass 10.2% of the north and 3.6% of the south.

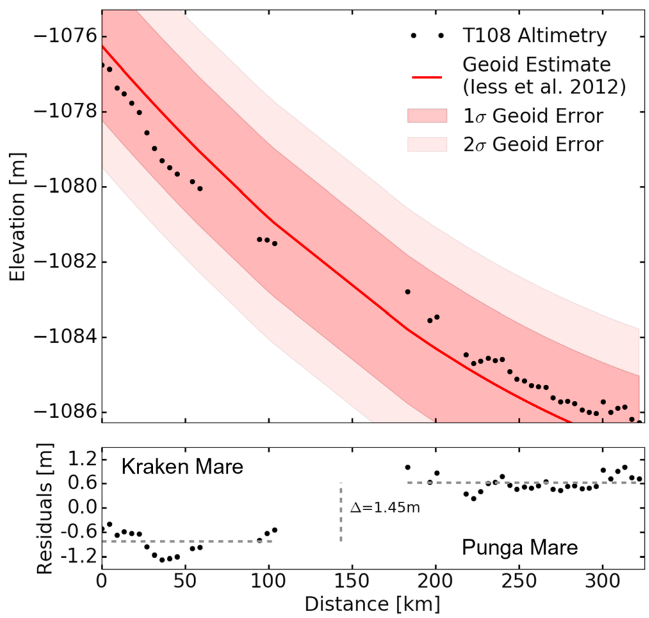

Figure 2. Altimetry height estimates of Punga and Kraken Mare from the January 2015 (T108) closest-approach altimetry pass. (top) The center of mass height estimates of specular bursts returned over the liquid surfaces plotted alongside the variability of the Iess et al. (2012) geoid for the burst center latitude and longitude positions. (bottom) The residuals obtained after subtracting sea surface elevations from the shape of the geoid. Within a given sea, the elevation estimates have a standard deviation of ~37 cm, consistent with the expected Cramer-Rao lower bound $\left(\sigma_h = {}^{c}/_{2B\sqrt{\mathrm{SNR}}} = 35 \text{ cm}\right)$ for a 40 dB signal (SNR = 10^4) and the 4.25 MHz bandwidth (B) of the Cassini RADAR altimeter. The two sea surfaces have an average geoid-corrected elevation difference of 1.4 m, which is considerably smaller than the 11 m variability of the Iess et al. (2012) geoid along the track.

The Cassini RADAR has observed Titan's polar regions in altimetry mode on eight occasions; 12 May 2007 (T30), 21 December 2008 (T49), 23 May 2013 (T91), 10 July 2013 (T92), 14 October 2013 (T95), 21 August 2014 (T104), 11 January 2015 (T108), and 15 April 2017 (T126). Six of these passes (T30, T49, T92, T104, T108, and T126) were acquired during the spacecraft's closest approach to Titan (1,200–2,000 km altitude), providing 3 dB footprint diameters of ~10 km on the surface. Collectively, these altimetry passes contain returns from the surfaces of Ligeia Mare, Kraken Mare, and Punga Mare, as well as Ontario Lacus and nine additional smaller liquid-filled SEDs. When referenced to the geoid determined by Iess et al. (2012), the liquid levels of the three north polar Mare are observed to be consistent to within 8 m, which is considerably smaller than the reported three-sigma residual ephemeris uncertainty of ~100 m (Stiles et al., 2009). Punga Mare and Kraken Mare, which were both observed during the T108 altimetry pass and not subject to pass-to-pass ephemeris uncertainties, can be constrained to be at the same elevation (geoid subtracted) to within ~1.4 m, which is considerably smaller than the 11 m of geoid variability expected across the 300 km portion of the altimetry track (Figure 2). Such an accurate vertical precision is made possible by the substantial (40 dB) signal-to-noise ratio (SNR) afforded by the specular reflections from the sea surface. To within error, the combined surfaces of the Maria are consistent with an equipotential surface, as previously predicted based on the elevation of shorelines determined by radargrammetry (e.g., Hayes et al., 2011; Kirk et al., 2008) and consistent with morphologic observations that the seas are connected (Sotin et al. 2012). In the following sections, we will use the average Mare liquid elevation (−927 m) as a reference for comparison with both filled and empty lacustrine basins. The 11 filled, and distant, lakes observed by altimetry have liquid levels several hundred meters above the seas (Figure 4 and Table S1 in the supporting information), suggesting that they reside in isolated or perched drainage basins that may or may not be hydraulically connected to the Mare. The implications of these findings are discussed below.

3. Sharp-Edged Depressions: Morphology

SEDs are found throughout the polar region and do not exhibit any obvious planview orientation or spatial patterns, such as forming along lines (Hayes et al., 2008). Dry SEDs have an average depth, relative to surrounding terrain, of 200 ± 100 m (1-sigma). There is no significant correlation between depth and planview size (Table S1 in the supporting information). Figure 1 shows the profiles of two SEDs observed during closest approach passes in March 2008 (T30) and April 2017 (T126). Michaelides et al. (2016) used Delay-Doppler processed altimetry (which increases along-track resolution) to reveal that the SED depicted in Figure 1a has wall slopes in excess of 45° and a raised rim that is elevated >300 m above the surrounding terrain. Filled SEDs observed during T126 showed similarly sized raised rims (Figure 1b). In fact, many, but not all, of the SEDs exhibit decameter to hectometer vertical-scale raised rims. Of the 15 SEDs observed by closest-approach altimetry, 13 have observable rims elevated >20 m relative to the surrounding terrain (with an average elevation of ~100 m). As the rims are relatively narrow (typically <1–5 km in spatial width), SAR-Topo and digital topographic models (DTMs), which have kilometer-scale or greater spatial resolution, can only resolve the largest of them. Of the remaining 71 north polar SEDs with topographic coverage (there are >600 total filled/empty north polar SEDs), 36 have clearly identifiable raised rims (Table S1 in the supporting information). In the south, 4 of 23 SEDs (there are >200 total, with all but a few being empty) have raised rims. These SEDs are found throughout both polar terrains (Figure S2 in the supporting information), arguing against any spatial preference for the presence or absence of a raised rim. Almost all SEDs with areas >750 km^2 have raised rims, emphasizing that not identifying a rim on smaller features could be a resolution effect. As with the example shown in Figure 1a, these rims are not always symmetric and can be found at variable elevations or be absent entirely on differing sides of a basin. When overlapping SAR image pairs containing these features are viewed in a stereoscopic display, many of the SEDs appear to be contained within broad convex domes.

Howard (1995) showed that the planform shape of geomorphic features, especially their planview curvature distribution, may constrain formation and evolution mechanisms. The planform shapes of Titan's SED basins exhibit a negatively skewed planform curvature (Figures 3d and 3e), consistent with expansion from one or more initial depressions through uniform scarp retreat. The negative skewness arises from the fact that inward facing protrusions are sharper and narrower than outward facing promontories. There is also a correlation between basin size and planview complexity, with some larger basins appearing to have been formed by agglomeration of several smaller features (Figure 3f). Many empty basin floors are relatively smooth but can show stepwise elevation variations in accordance with planform complexity. There majority of these basins exhibit no observable blocks, fractures, or slumps at the ~300 m resolution of Cassini SAR images.

In general, Titan's SEDs represent topographically closed depressions (Figures 3a–3c) with no evidence, at the 300 m resolution of SAR images, of terrain features that would suggest inflow or outflow of fluid on the surface (e.g., channels) or overflow/spillage into surrounding terrain (e.g., alluvial fans). Figure 4 shows the elevation of SED floors relative to Mare liquid levels measured where basin floors intersected available topographic data. Basin depths, as compared to immediately surrounding terrain, are represented by the length of each bar and range from the detectability limit of ~100 m to a maximum observed depth of $>$600 m. Basin depths differ and appear to be positively correlated with the surface elevation of the undulating plains into which the SEDs are inset. Within the drainage basins containing the northern Mare, the absolute elevations of empty basin floors are, to within error, always above the Mare liquid level (Figure 4). Similarly, the floor elevations of empty SEDs appear to be, to within error, above the liquid surface elevation of filled SEDs within the same drainage basins (color groupings in Figures 4 and S2 in the supporting information, see Birch et al., 2017, for basin definitions). Basins with floors closer to the local phreatic surface appear brighter to both nadir and off-nadir microwave observations than those that are more elevated, indicating a potential change in exposed material composition or state of liquid saturation. The same pattern holds for the southern hemisphere, with the liquid level of Ontario Lacus lying below the floor elevations of all southern SEDs (Figure 4).

Figure 4 demonstrates that dry SEDs are not found with floor elevations that reach below the local liquid elevation (where measured) within a given topographic basin. Presumably, depressions with floors that are below either the Mare or local perched liquid elevations would fill with liquid. The eleven liquid-filled SEDs for which we have altimetry measurements indicate that liquid levels can differ from basin to basin. In between basins, the aquifers may be sloping (e.g., the Ogallala aquifer of the U.S. Great Plains, whose predevelopment water table varies by 1,300 m over the 1,000 km between Colorado and Nebraska (Loaiciga, 2005, Steward & Allen, 2016)) or interrupted by impermeable materials.

4. Mechanistic Constraints

The relatively flat floors, significant depth, and lack of observable evidence for inflow or outflow channels through Titan's SEDs create a mass conservation problem, as basin formation requires significant removal of material. Removing material from topographically closed basins typically requires either sublimation, similar to the formation of Swiss Cheese Terrain in the south polar ice cap of Mars (Bibring et al., 2004; Thomas et al., 2005), or dissolution and removal via subsurface fluid flow, such as in the formation of the sinkhole lakes in the Florida Everglades (Gerould & Higer, 1999) or salt collapse basins in Bottomless Lakes State Park New Mexico (Land, 2006) and along the shores of the Dead Sea (Yechieli et al., 2006). While Aeolian processes are known to generate some terrestrial basins, such as Yihezhagedehaizi Lake in the Badanjilin Desert of China (Pachur et al., 1995), they are typically very shallow ($<$10 m deep), small ($<$2 km^2), and surrounded by other aeolian morphologies (e.g., dunes). While winds are strong enough to create dunes in Titan's equatorial terrain, typical polar winds are predicted to be light ($<$1 m/s; Hayes et al., 2013) and no aeolian features have been reliably identified in polar terrain, although yardangs have been proposed at high midlatitudes (Radebaugh, 2013).

Dissolution and/or sublimation processes require a polar regolith to contain a sufficient fraction of volatile material to permit formation of basins with depths of up to ~500 m. Water ice is both stable in Titan's atmosphere and insoluble in liquid methane/ethane (Lorenz & Lunine, 1996; Perron et al., 2006) and is thought to

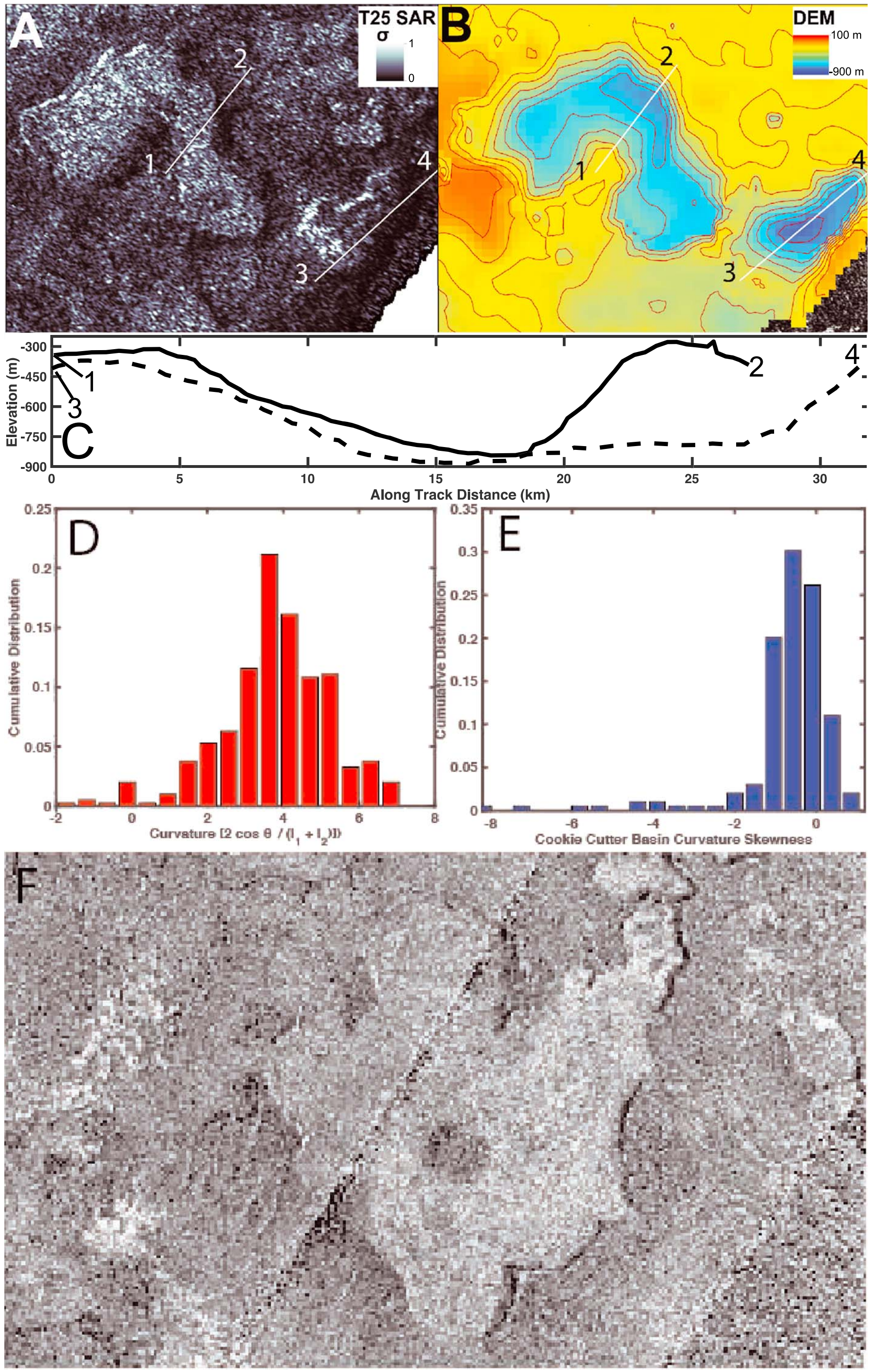

Figure 3. (a) SAR image and (b) DTM of an unfilled and partially filled SED observed in February and April 2007. (c) The topographic profiles show that both reach similar depths, with the partially filled feature extending 42 m deeper. (d) The curvature distribution of the larger basin depicted in Figure 3a. (e) The distribution has a negative skewness, similar to majority of SEDs, as shown in the distribution of basin curvature skewness for all SEDs. (f) An example of a complex SED that appears to have been generated by agglomeration of several smaller features. The dark area in the center of the basin is topographically high.

underlie the surface, but cannot thus be eroded by dissolution or sublimation. To create an erodible material, a significant amount of volatiles must have been delivered to Titan's poles through processes other than uniform deposition of atmospherically derived photolysis products, which are predicted to deliver a material volume with a global precipitable column depth of ~10 m of solid organics (Krasnopolsky, 2010;

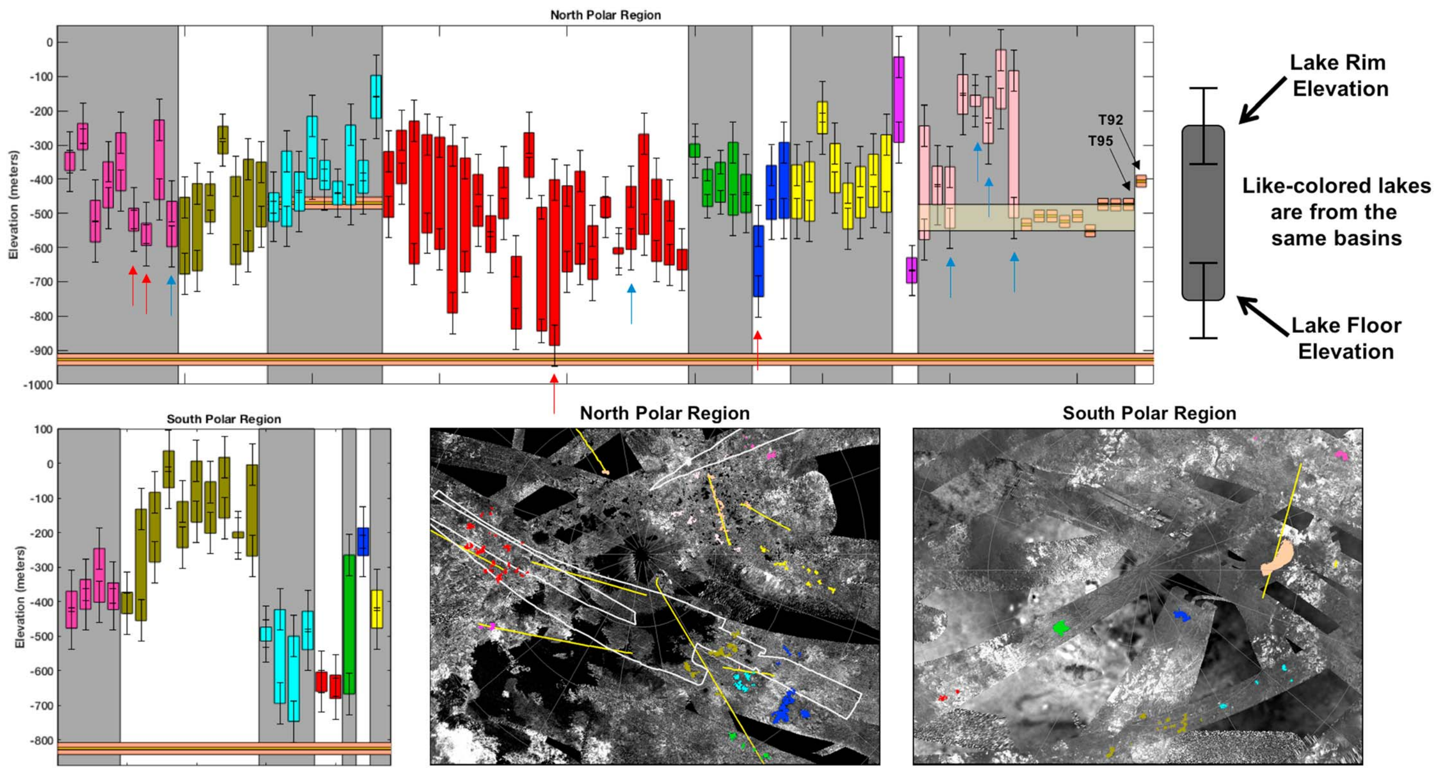

Figure 4. Distribution of SED elevations in the (top) north and (bottom) south polar regions of Titan. For each basin, the bottom of the bar represents the floor elevation and the top represents the elevation of surrounding terrain. Within a given drainage basin (denoted by color groupings, Figure S2 in the supporting information, see Birch et al., 2017), unfilled basin floors appear above observed liquid elevations (to within error). Note that the filled SEDs (i.e., lakes) have liquid elevations that are hundreds of meters above the elevation of the Mare. The blue (high confidence) and red (lower confidence) arrows correspond to basins that appear have liquid in a portion of their bottoms. Some SEDs show stepwise topography, and the reported elevation is the lowest (dry) step intersected by topographic data. Liquid elevations of filled SEDs, measured by altimetry, are depicted by orange bars. The Mare elevation is shown as an orange horizontal bar at −927 m and Ontario Lacus is measured at −825 m.

Lavvas et al., 2008). Brown et al. (2006), for example, suggested that acetylene and other volatile organics may have preferentially transported from Titan's equator to its poles over geologic time to form volatile caps. Recently, the Visual and Infrared Mapping Spectrometer and Infrared Science Subsystems instruments on Cassini identified bright deposits around Titan's poles that may indicate compositional variability and appear to correlate with the undulating plains observed by RADAR (Birch et al., 2017). Alternatively, large amounts of volatile material could have been deposited by evaporation of large ancient polar oceans, although it is unclear where the fluid in these oceans would have come from (see Birch et al., 2017).

The negative skewness in the curvature of SED planview boundaries is indicative of uniform scarp retreat (Howard, 1990; Moore & Howard, 2011). The most common ways to retreat a scarp are to undermine (a) erodible material beneath a resistant surface layer, such as the Colorado Plateau (Schmidt, 1989) or scarps of the Kentucky Karst (Able, 1986); (b) basal slope erosion, such as what occurs during shoreline retreat along marine cliff faces in the presence of wave erosion (Dietz, 1963); or (c) bi-stable erosion and deposition similar to the generation of stepped topography in the Martian polar layered terrain (Howard, 1978). The complex form and stepwise floor topography of the larger SEDs are consistent with agglomeration of smaller retreating features (Figure 3d). Such retreat would have to be coupled with processes removing excavated material and creating relatively flat floors.

Perhaps the most mechanistically constraining observation regarding Titan's SEDs is the hundred-meter scale raised rims associated with a subset of the features. The most straightforward way to generate a raised rim is for it to be a natural by-product of basin formation. For example, if lakes started out as topographic domes that form central defects that grow through outward scarp retreat, the remnants of the dome would form a raised rim. This is analogous to the formation of pingos. Similarly, erosion by sublimation followed by reprecipitation of volatiles can generate pits with raised rims, a process analogous to the formation of penitentes on Callisto (White et al., 2016). Thermodynamically, sublimation erosion is difficult given the lack of significant temperature gradients (Cottini et al., 2012) and the scarcity of known volatile species on Titan's surface today. Raised rims could also be formed through uplift, such as what would occur if interactions between the wall material and atmosphere/fluid caused a volume change similar to swelling clay or hydration of anhydrite ($CaSO_4$) to form gypsum ($CaSO_4 \cdot 2H_2O$) (Young & Smith, 2000). This is not likely given the material properties of the water ice and solid organics believed to make up Titan's polar terrain (Cornet et al., 2015; Perron et al., 2006). Fluid overflow could result in precipitated rims similar to fluvial levees, although the asymmetric nature of some raised rims appear to preclude such a mechanism in the absence of differential erosion. Finally, the rims could represent lithified or armored annuli that are exposed as erosion deflates surrounding terrain, similar to the process of forming inverted channels (Williams et al., 2009), which could potentially form through chemical case-hardening of surrounding materials (Malaska & Hodyss, 2014).

No systematic morphological features have been observed in association with SEDs that are suggestive of structural deformation (e.g., interior slump structures, radial or concentric lineations exterior to the basin, or systematic elongation or alignment of SEDs).

5. Discussion

A complete model for the formation of Titan's SED basins needs to explain the origin of the undulating plains, generation of initial depressions, or seed points, in the undulating plains, negatively skewed planform that implies growth through uniform scarp retreat and depression agglomeration, relatively flat floors that imply significant mass removal, formation of raised rims, and their ultimate hectometer depths and tens of kilometer-scale diameters. Formation cannot involve significant fluvial processes unless the widths of the resulting channels and/or valleys remain smaller than the ~300 m resolution of the Cassini RADAR. Regardless, fluvial channels cannot be the dominant method for removing material from the basin. Within a regional topographic basin, the lakes appear dynamically linked such that their fill state is determined by the elevation of their basin floors as compared to the local phreatic surface or impermeable boundary. Spatially, formation models should not generate preferential orientations in planview expression or create distributions that suggest significant structural control. Finally, the basins must only encompass a relatively minor fraction (~12%) of the exposed undulating plains, constraining the rate of depression formation to be slow relative to the rate and/or frequency of any resurfacing mechanisms.

The above constraints challenge almost any formation model. While cryovolcanism could work for a minor subset of small topographically raised features described by Wood et al. (2010), the SEDs require a net removal process. Furthermore, caldera collapse and/or explosion craters are not known to form raised rims. A cryovolcanic interpretation would also fail to account for expansion through uniform scarp retreat, although cryovolcanic processes may act as seed points for initial formation with subsequent growth dominated by other mechanisms. Similarly, other doming mechanisms such as organic diapirs (e.g., terrestrial salt domes), spring mounds, or karst-driven isostasy (Woo et al., 2017) may also contribute. The noncircular shapes and dense spatial clustering argues against impact craters, although impacts cannot be ruled out as another potential seeding mechanism. Though periglacial processes may produce features with analogous three-dimensional forms on Earth (e.g., pingos), their formation on Titan are thermodynamically discouraged given the apparent absence of volume change processes equivalent to terrestrial freeze-thaw cycles (e.g., Choukroun et al., 2010). Similarly, glacial processes are unlikely considering the absence of large blocks of solid hydrocarbon (methane, ethane, ethylene, and acetylene) that could be mobilized and then revolatilized or removed under the current Titan temperatures. While glacial and/or tectonic processes may have been more prevalent under a past climate or chemical regime, there are no obvious morphologic indicators that these processes were important in forming the SED basins. Finally, gas pockmarks (Cathles et al., 2010), such as those that form abundantly along the seafloor of the Gulf of Mexico, are morphologically and topographically similar to Titan's SEDs. Pockmarks, however, require significant volumes of gas in the near subsurface and it is unclear what the gas source would be on Titan.

The mechanisms that fit the observations best are either dissolution or sublimation of a volatile substrate that underlies a more resistant cap layer, although a lack of significant temperature gradients makes sublimation erosion difficult to reconcile in the current climate regime. These two models are compatible with uniform scarp retreat of a steep-sided depression that has no observable inflow or outflow channels. A challenge to these formation mechanisms is the presence of raised rims, which are a feature not seen in traditional karstic terrain, although may be explained by a process analogous to pingo or Uvala formation. As with all potential formation mechanisms, sublimation and dissolution also struggle with conserving sediment mass. Comparatively, terrestrial karst (up to ~250 m × 0.15 km^2 at Crveno Jezero in Croatia; Garasic & Jurkovic, 2012) and Mars' swiss-cheese terrain (~8 m × 0.01 km^2; Thomas et al., 2000) morphologies are orders of magnitude smaller in size than the depressions on Titan (~600 m × 70 km^2). Since mass removal is proportional to the volume of the cavity, a dissolution/sublimation model for Titan's SEDs requires ~10^3–10^6 times more material to move through the subsurface or sublimate into the atmosphere than is typical for formation of morphologically similar (but smaller) features observed on the Earth and Mars. We note, however, that sublimation features on other bodies (e.g., hollows on Mercury (Blewett et al., 2011) and pits on Pluto (Moore et al., 2017)) can be very large if sublimation rates are relatively low and material strength is comparatively high.

Acknowledgments
A.G.H., W.E.D., A.D.H., R.L.K., and R.L.M. acknowledge the support of NASA Cassini Data Analysis Program (CDAP) grant NNX13AG03G and NASA Early Career Fellowship grant NNX14AJ57G. S.P.D. and P.M.C. acknowledge the support of NESSF grants NNX15Q87H and NNX14AQ31H, respectively. M.M. and V. P. acknowledge the support of NASA CDAP grant NNX15AH10G. R.D.L. acknowledges the support of NASA Outer Planets Research grant NNX13AK97G. The research was carried out in-part at the Jet Propulsion Laboratory, California Institute of Technology, under a contract with the National Aeronautics and Space Administration. The topographic data used to measure SED and Mare elevations are available in the supporting information of Corlies et al. (2017). Shapefiles for SED and Mare boundaries can be obtained from the supporting information of Birch et al. (2017). Both data sets are also available at http://hayesresearchgroup.com/data-products/. Derived SED and Mare elevations are listed in Table S1 in the supporting information to this manuscript.

References

Able, A. (1986). *Karstification of the Pennyroyal Plain behind the retreating Chester Escarpment: Warren, Simpson & Logan Counties*. Kentucky: Western Kentuck University.

Aharonson, O., Hayes, A., Hayne, P., Lopes, R., Lucas, A., & Perron, J. (2014). Titan's surface geology. In I. Müller-Wodarg, C. Griffith, E. Lellouch, & T. Cravens (Eds.), *Titan: Interior, Surface, Atmosphere, and Space Environment, Cambridge Planetary Science* (pp. 63–101). Cambridge: Cambridge University Press. https://doi.org/10.1017/CBO9780511667398.005

Aharonson, O., Hayes, A. G., Lunine, J. I., Lorenz, R. D., Allison, M. D., & Elachi, C. (2009). An asymmetric distribution of lakes on Titan as a possible consequence of orbital forcing. *Nature Geoscience*, *2*(12), 851–854. https://doi.org/10.1038/ngeo698

Bibring, J. P., Langevin, Y., Poulet, F., Gendrin, A., Gondet, B., Berthé, M., … OMEGA team (2004). Perennial water ice identified in the south polar cap of Mars. *Nature*, *428*(6983), 627–630. https://doi.org/10.1038/nature02461

Birch, S. P. D., Hayes, A. G., Dietrich, W. E., Howard, A. D., Bristow, C. S., Malaska, M. J., … Lopes, R. M. C. (2017). Geomorphologic mapping of titan's polar terrains: Constraining surface processes and landscape evolution. *Icarus*, *282*, 214–236. https://doi.org/10.1016/j.icarus.2016.08.003

Blewett, D. T., Chabot, N. L., Denevi, B. W., Ernst, C. M., Head, J. W., Izenberg, N. R., … Hurwitz, D. M. (2011). Hollows on Mercury: MESSENGER evidence for geologically recent volatile-related activity. *Science*, *333*(6051), 1856–1859. https://doi.org/10.1126/science.1211681

Brown, R. H., Griffith, C. A., Lunine, J. I., & Barnes, J. W. (2006). Polar caps on Titan? In *European Planetary Science Congress* 2006 (pp. 602).

Cathles, L. M., Su, Z., & Chen, D. F. (2010). The physics of gas chimney and pockmark formation, with implications for assessment of seafloor hazards and gas sequestration. *Marine and Petroleum Geology*, *27*, 82–91. https://doi.org/10.1016/j.marpetgeo.2010.01.004

Choukroun, M., Grasset, O., Tobie, G., & Sotin, C. (2010). Stability of methane clathrate hydrates under pressure: Influence on outgassing processes of methane on Titan. *Icarus*, *205*(2), 581–593. https://doi.org/10.1016/j.icarus.2009.08.011

Corlies, P., Hayes, A. G., Birch, S., Lorenz, R., Stiles, B. W., Kirk, R., … Iess, L. (2017). Titan's topography and shape at the end of the Cassini mission. *Geophysical Research Letters*, *44*. https://doi.org/10.1002/2017GL075518

Cornet, T., Cordier, D., Le Bahers, T., Bourgeois, O., Fleurant, C., Mouélic, S. L., & Altobelli, N. (2015). Dissoution on Titan and on Earth: Toward the age of Titan's karstic landscapes. *Journal of Geophysical Research: Planets*, *120*, 1044–1074. https://doi.org/10.1002/2014JE004738

Cottini, V., Nixon, C. A., Jennings, D. E., de Kok, R., Teanby, N. A., Irwin, P. G. J., & Flasar, F. M. (2012). Spatial and temporal variations in Titan's surface temperatures from Cassini CIRS observations. *Planetary and Space Science*, *60*(1), 62–71. https://doi.org/10.1016/j.pss.2011.03.015

Dietrich, W. E., Bellugi, D. G., Sklar, L. S., Stock, J. D., Heimsath, A. M., & Roering, J. J. (2013). Geomorphic transport laws for predicting landscape form and dynamics. In P. R. Wilcock & R. M. Iverson (Eds.), *Prediction in geomorphology* (pp. 103–132). Washington, DC: American Geophysical Union.

Dietz, R. S. (1963). Wave-base, marine profile of equilibrium, and wave-built terraces—A critical appraisal. *Geological Society of America Bulletin*, *74*(8), 971. https://doi.org/10.1130/0016-7606(1963)74%5B971:WMPOEA%5D2.0.CO;2

Garasic, V., & Jurkovic, I. (2012). Geochemical characteristics of different iron ore types from the Southern Tomasica deposit, Ljubija, NW Bosnia. *Geologia Croatica*, *65*, 255–270.

Gerould, S., & Higer, A. (1999). U.S. Geological Survey program on the South Florida ecosystem. In *Proceedings of South Florida restoration science forum, May 17–19, 1999* (Rep. 99–181). Boca Raton, FL.

Hayes, A., Aharonson, O., Callahan, P., Elachi, C., Gim, Y., Kirk, R., … Wall, S. (2008). Hydrocarbon lakes on Titan: Distribution and interaction with a porous regolith. *Geophysical Research Letters*, *35*, L09204. https://doi.org/10.1029/2008GL033409

Hayes, A. G. (2016). Titan's lakes and seas. *Annual Review of Earth and Planetary Sciences*, *44*(1), 57–83. https://doi.org/10.1146/annurev-earth-060115-012247

Hayes, A. G., Aharonson, O., Lunine, J. I., Kirk, R. L., Zebker, H. A., Wye, L. C., … the Cassini RADAR Team (2011). Transient surface liquid in Titan's polar regions from Cassini. *Icarus*, *211*(1), 655–671. https://doi.org/10.1016/j.icarus.2010.08.017

Hayes, A. G., Lorenz, R. D., Donelan, M. A., Manga, M., Lunine, J. I., Schneider, T., … Notarnicola, C. (2013). Wind driven capillary-gravity waves on Titan's lakes: Hard to detect or non-existent? *Icarus*, *225*(1), 403–412. https://doi.org/10.1016/j.icarus.2013.04.004

Howard, A. D. (1978). Origin of stepped topography of Martian poles. *Icarus*, *34*(3), 581–599. https://doi.org/10.1016/0019-1035(78)90047-7

Howard, A. D. (1990). Role of hypsometry and planform in basin hydrologic response. *Hydrological Processes*, *4*(4), 373–385. https://doi.org/10.1002/hyp.3360040407

Howard, A. D. (1995). Simulation modeling and statistical classification of escarpment planforms. *Geomorphology*, *12*(3), 187–214. https://doi.org/10.1016/0169-555X(95)00004-O

Iess, L., Jacobson, R. A., Ducci, M., Stevenson, D. J., Lunine, J. I., Armstrong, J. W., … Tortora, P. (2012). The tides of Titan. *Science*, *337*(6093), 457–459. https://doi.org/10.1126/science.1219631

Kirk, R. L., Howington-Kraus, E., Stiles, B. W., & Hensley, S. (2008). Digital topographic models of Titan produced by RADAR stereogrammetry with a rigorour sensor model. Presented at Lunar and Planetary Science XXXIX.

Krasnopolsky, V. A. (2010). The photochemical model of Titan's atmosphere and ionosphere: A version without hydrodynamic escape. *Planetary and Space Science*, *58*(12), 1507–1515. https://doi.org/10.1016/j.pss.2010.07.010

Land, L. (2006). Hydrogeology of Bottomless Lakes State Park. *New Mexico Geological Society Guidebook*, *57*, 95–96.

Lavvas, P. P., Coustenis, A., & Vardavas, I. M. (2008). Coupling photochemistry with haze formation in Titan's atmosphere. Part I: Model description. *Planetary and Space Science*, *56*(1), 27–66. https://doi.org/10.1016/j.pss.2007.05.026

Loaiciga, H. A. (2005). Steady state phreatic surfaces in sloping aquifers. *Water Resources Research*, *41*, W08402. https://doi.org/10.1029/2004WR003861

Lorenz, R. D., & Lunine, J. I. (1996). Erosion on Titan: Past and present. *Icarus*, *122*(1), 79–91. https://doi.org/10.1006/icar.1996.0110

Malaska, M. J., & Hodyss, R. (2014). Dissolution of benzene, naphthalene, and biphenyl in a simulated Titan lake. *Icarus*, *242*, 74–81. https://doi.org/10.1016/j.icarus.2014.07.022

Michaelides, R. J., Hayes, A. G., Mastrogiuseppe, M., Zebker, H. A., Farr, T. G., Malaska, M. J., … Mullen, J. P. (2016). Constraining the physical properties of Titan's empty lake basins using nadir and off-nadir Cassini RADAR backscatter. *Icarus*, *270*, 57–66. https://doi.org/10.1016/j.icarus.2015.09.043

Moore, J. M., & Howard, A. D. (2011). Are the basins of Titan's Hotei Regio and Tui Regio sites of former low latitude seas? *Geophysical Research Letters*, *38*, L04201. https://doi.org/10.1029/2010GL045234

Moore, J. M., Howard, A. D., & Morgan, A. M. (2014). The landscape of Titan as witness to its climate evolution. *Journal of Geophysical Research: Planets*, *119*, 2060–2077. https://doi.org/10.1002/2014JE004608

Moore, J. M., Howard, A. D., Umurhan, O. M., White, O. L., Schenk, P. M., Beyer, R. A., … Ennico, K. (2017). Sublimation as a landform-shaping process on Pluto. *Icarus*, *287*, 320–333. https://doi.org/10.1016/j.icarus.2016.08.025

Pachur, H. J., Wunnemann, B., & Zhang, H. (1995). Lake evolution in the Tengger Desert, Northwestern China, during the last 40,000 years. *Quaternary Research*, *44*(02), 171–180. https://doi.org/10.1006/qres.1995.1061

Perron, J. T., Lamb, M. P., Koven, C. D., Fung, I. Y., Yager, E., & Adamkovics, M. (2006). Valley formation and methane precipitation rates on Titan. *Journal of Geophysical Research*, *111*, E11001. https://doi.org/10.1029/2005JE002602

Radebaugh, J. (2013). Dunes on Saturn's moon Titan as revealed by the Cassini mission. *Aeolian Research*, *11*, 23–41. https://doi.org/10.1016/j.aeolia.2013.07.001

Schmidt, K. H. (1989). The significance of scarp retreat for Cenozoic landform evolution on the Colorado Plateau, USA. *Earth Surface Processes and Landforms*, *14*(2), 93–105. https://doi.org/10.1002/esp.3290140202

Sotin, C., Lawrence, K. J., Reinhardt, B., Barnes, J. W., Brown, R. H., Hayes, A. G., … Stephan, K. (2012). Observations of Titan's Northern lakes at 5 μm: Implications for the organic cycle and geology. *Icarus*, *221*, 768–786. https://doi.org/10.1016/j.icarus.2012.08.017

Steward, D. R., & Allen, A. J. (2016). Peak groundwater depletion in the High Plains Aquifer, projections from 1930 to 2110. *Agricultural Water Management*, *170*, 36–48. https://doi.org/10.1016/j.agwat.2015.10.003

Stiles, B. W., Hensley, S., Gim, Y., Bates, D. M., Kirk, R. L., Hayes, A., … Veeramacheneni, C. (2009). Determining Titan surface topography from Cassini SAR data. *Icarus*, *202*(2), 584–598. https://doi.org/10.1016/j.icarus.2009.03.032

Stofan, E. R., Elachi, C., Lunine, J. I., Lorenz, R. D., Stiles, B., Mitchell, K. L., … West, R. (2007). The lakes of Titan. *Nature*, *445*(7123), 61–64. https://doi.org/10.1038/nature05438

Thomas, P. C., Malin, M. C., Edgett, K. S., Carr, M. H., Hartmann, W. K., Ingersoll, A. P., … Sullivan, R. (2000). North-south geological differences between the residual polar caps on Mars. *Nature*, *404*(6774), 161–164. https://doi.org/10.1038/35004528

Thomas, P. C., Malin, M. C., James, P. B., Cantor, B. A., Williams, R. M. E., & Gierasch, P. (2005). South polar residual cap of Mars: Features, stratigraphy, and changes. *Icarus*, *174*(2), 535–559. https://doi.org/10.1016/j.icarus.2004.07.028

White, O. L., Umurhan, O. M., Moore, J. M., & Howard, A. D. (2016). Modeling of ice pinnacle formation on Callisto. *Journal of Geophysical Research: Planets*, *121*, 21–45. https://doi.org/10.1002/2015JE004846

Williams, R. M. E., Irwin, R. P., & Zimbelman, J. R. (2009). Evaluation of paleohydrologic models for terrestrial inverted channels: Implications for application to martian sinuous ridges. *Geomorphology*, *107*(3-4), 300–315. https://doi.org/10.1016/j.geomorph.2008.12.015

Woo, H. B., Panning, M. P., Adams, P. N., & Dutton, A. (2017). Karst-driven flexural isostacy in North-Central Florida. *Geochemistry, Geophysics, Geosystems*, *18*, 3327–3339. https://doi.org/10.1002/2017GC006934

Wood, C. A., Lorenz, R., Kirk, R., Lopes, R., Mitchell, K., & Stofan, E. (2010). Impact craters on Titan. *Icarus*, *206*(1), 334–344. https://doi.org/10.1016/j.icarus.2009.08.021

Yechieli, Y., Abelson, M., Bein, A., Crouvi, O., & Shtivelman, V. (2006). Sinkhole "swarms" along the Dead Sea coast: Reflection of disturbance of lake and adjacent groundwater systems. *Geological Society of America Bulletin*, *118*(9-10), 1075–1087. https://doi.org/10.1130/B25880.1

Young, D. A., & Smith, D. E. (2000). Simulations of clay mineral swelling and hydration: Dependence upon interlayer ion size and charge. *Journal of Physical Chemistry B*, *104*(39), 9163–9170. https://doi.org/10.1021/jp000146k